Chapter 4. Cluster Phase Chemistry: Gas Phase Reactions of Anionic Sodium Salts of Dicarboxylic Acid Clusters with Water Molecules

Reproduced with permission from Kim, H. I.; Goddard, W. A.; Beauchamp, J. L. *J. Phys. Chem. A*, **2006**, *110*, 7777. Copyright 2006 American Chemical Society.

4.1. Abstract

A homologous series of anionic gas phase clusters of dicarboxylic acids (oxalic acid, malonic acid, succinic acid, glutaric acid, and adipic acid) generated via electrospray ionization (ESI) are investigated using collision induced dissociation (CID). Sodiated clusters with the composition $(Na^{+})_{2n+1}(\text{dicarboxylate}^{2-})_{n+1}$ for singly charged anionic clusters, where n = 1-4, are observed as major gas phase species. Isolation of the clusters followed by CID results mainly in sequential loss of disodium dicarboxylate moieties for the clusters of succinic acid, glutaric acid, and adipic acid (C4-C6). However, all oxalate (C2) and malonate (C3) clusters and dimers (n = 1) of succinate (C4) and glutarate (C5) exhibit more complex chemistry initiated by collision of the activated cluster with water molecules. For example, with water addition, malonate clusters dissociate to yield sodium acetate, carbon dioxide, and sodium hydroxide. More generally, water molecules serve as proton donors for reacting dicarboxylate anions in the cluster and introduce energetically favorable dissociation pathways not otherwise available. Density functional theory (DFT) calculations of the binding energy of the cluster correlate well with the cluster phase reactions of oxalate and malonate clusters. Clusters of larger dicarboxylate

ions (C4-C6) are more weakly bound, facilitating the sequential loss of disodium dicarboxylate moieties. The more strongly bound small dicarboxylate anions (oxalate and malonate) preferentially react with water molecules rather than dissociate to lose disodium dicarboxylate monomers when collisionally activated. Implications of these results for the atmospheric aerosol chemistry of dicarboxylic acids are discussed.

4.2. Introduction

Dicarboxylic acids are found in tropospheric aerosols in both continental and marine environments.[1-7] Dicarboxylic acids with high molecular weight (C20-C32) in the aerosol are produced via direct transport from organic material in soil.[1] However, small dicarboxylic acids have been considered to be the products from photo induced oxidation of unsaturated hydrocarbons in the gas phase.[1,5,8] These small dicarboxylic acids are important as significant contributors of organic material mass in atmospheric aerosols.[5,6,9,10] Early studies clearly document the important role of clusters in atmospheric aerosol chemistry.[11] Gas phase dicarboxylic acids can aggregate with sodium cation, which is a major component of sea salt particles in the atmosphere,[12,13] forming sodium-dicarboxylic acid clusters.

Previous studies of the atmospheric chemistry of dicarboxylic acids have suggested that decarboxylation processes can be photo induced.[14-16] The intramolecular cyclic transition state structure is a well-known unimolecular decarboxylation pathway of oxalic acid and malonic acid.[14,15] Donaldson and co-workers have reported several studies of atmospheric reactions involving water complex formation,[16-19] including theoretical investigations of the decarboxylation of malonic acid via formation of a malonic acid-water complex.[16] Staikova et al. report that addition of a water molecule to malonic acid lowers the decarboxylation barrier overall by ~10 kcal/mol.[16] The water molecule is used as a catalyst in the decarboxylation of such complexes. The water accepts an acidic proton from one carboxyl group and transfers a proton to the carbonyl of the other acid group to facilitate the decarboxylation process.[16] The suggested mechanism for the decarboxylation of malonic acid via formation of the water-malonic acid complex by Staikova et al.[16] is shown in Scheme 1. However, there is no experimental evidence for this process.

Using the technique of electrospray ionization (ESI) to generate molecular clusters, we have recently initiated a general study of collisionally activated reactions that occur between cluster components, other than simple dissociations.[20-22] These studies have demonstrated that ionic clusters are a rich source of interesting chemical reactions that can be initiated by collisional activation. For example, Julian and Beauchamp have demonstrated the gas phase synthesis of ATP from clusters of the sodium salt of AMP.[21] Hodyss et al. have reported a range of S_N2 and E2 reactions of tetraalkylammonium ions with triphosphate and DNA anions via cluster formations in gas phase.[20] Recently, Cox et al. have demonstrated the phosphorylation of alcohols via cluster phase reactions of triphosphate and molecules possessing hydroxyl functional groups, with the selective phosphorylation of serine in a decapeptide as an interesting example.[22] Other groups have also made important contributions to this field study.[23-26]

In the present chapter, we generate strongly bound anionic gas-phase sodiated clusters of dicarboxylic acids (oxalic acid, malonic acid, succinic acid, glutaric acid, and adipic acid, Figure 1) via ESI. The cluster phase reactions of these molecular aggregates are investigated using ion trap mass spectrometry (ITMS) and collisional activation. Computational modeling of the structures of the reactants and products is performed in

Scheme 1. Reaction mechanism for the decarboxylation of malonic acid via water-malonic acid complex suggested by Staikova et al.[16]

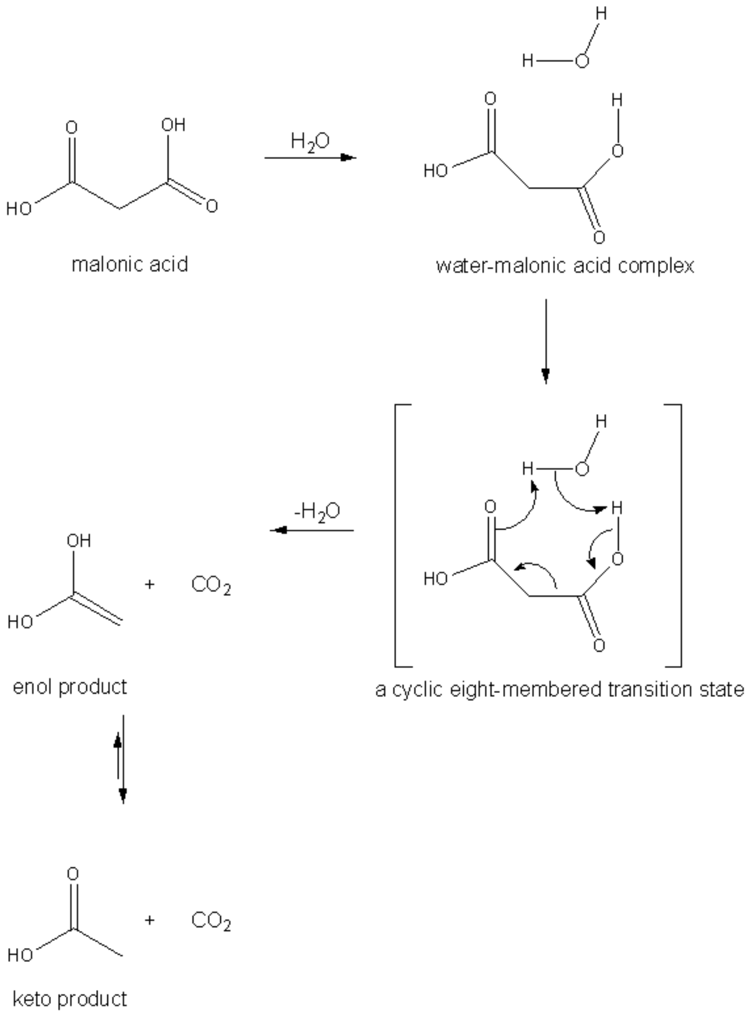

Figure 1. Homologous series of small dicarboxylic acids (C_2-C_6) examined in this study.

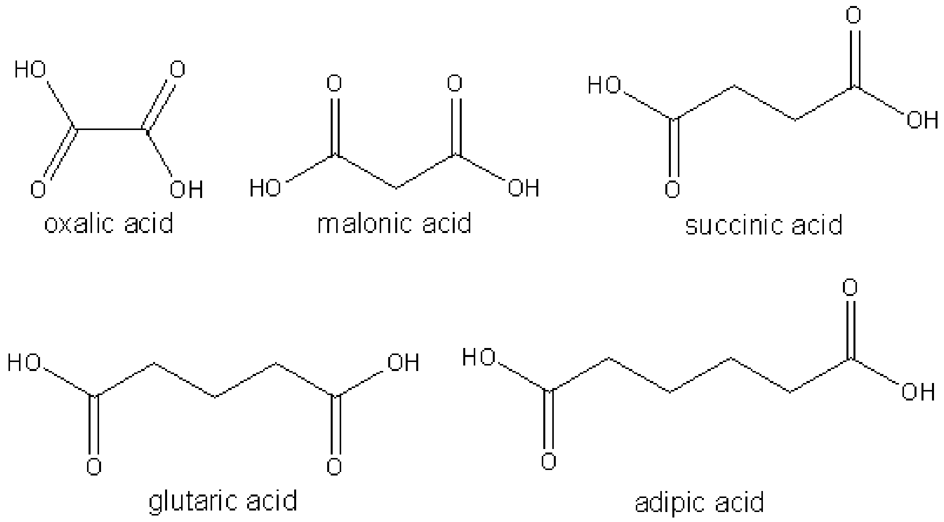

oxalic acid

malonic acid

succinic acid

glutaric acid

adipic acid

order to evaluate the mechanisms and energetics of observed reactions. Of particular interest are a range of dissociation reactions that are triggered by the bimolecular interaction of collisionally activated clusters with water molecules.

4.3. Experimental

Oxalic acid, malonic acid, succinic acid, glutaric acid, adipic acid, disodium malonate, disodium succinate, and sodium chloride were purchased from Sigma Chemical Company (St. Louis, MO) and used without further purification. All solvents (water and methanol) are HPLC grade and were purchased from J. T. Baker (Phillipsburg, NJ). For the sodium dicarboxylate studies, samples were prepared by dissolving stoichiometric amounts of sodium chloride and the dicarboxylic acid in a 50:50 methanol/water mixture by volume except for the malonate and succinate samples, which were purchased as the disodium salts. For comparison, samples without sodium chloride were prepared by dissolving a known quantity of dicarboxylic acid in a 50:50 methanol/water mixture by volume. Total sample concentrations were varied over the range 100–180 μM.

Experiments are performed on a Finnigan LCQ Deca ITMS in negative mode without further modification. Electrospray voltage of -5 kV, capillary voltage of -15 V, tube lens offset of -30 V, and capillary temperature in the range 200-300 °C are set as parameters for ESI. The temperature of the MS analyzer was measured as ~23 °C before the experiment and ~24 °C during the experiment. The pressure is estimated to be $\sim 10^{-3}$ torr He inside the trap. Under the assumption that water vapor, which is from internal surface outgassing and ESI solvent, is the dominant gas species in vacuum other than He,[27,28] water pressure in the trap was estimated as $\sim 10^{-6}$ torr. Cluster ions of interest were isolated and fragmented via collision induced dissociation (CID).[29] Dissociation of an ion by CID in an ion trap is normally described as a two-step phenomenon.[29] The ion becomes excited by transfer of a fraction of the ion's kinetic energy into internal modes in multiple collisions with inert He gas molecules inside of the ion trap. At a sufficiently high level of internal excitation, dissociation of the ion occurs. Since there is a delay between these two steps, reactions of excited ionic complexes can occur in collisions with neutral molecules rather than dissociation to yield monomers. The time between CID and detection is typically ~10 msec. This is sufficient time for activated ions to undergo bimolecular collisions with a water molecule with high probability. Continuous isolation of the cluster ions followed by CID (MS^n) is performed until the track of the isolated ion is lost. As will be shown below, bimolecular interaction with water molecules can play an important role in triggering the dissociation of a collisionally activated cluster.

Several candidate low energy structures of the reactants and products of observed reactions were evaluated at the PM5 level using CAChe 6.1.10 (Fujitsu, Beaverton, OR). Then, the lowest-energy structures were determined using density functional theory (DFT) with PM5 calculated structures. DFT calculations were performed using Jaguar 6.0 (Schrödinger, Portland, OR) utilizing the Becke three-parameter functional (B3)[30] combined with the correlation functional of Lee, Yang, and Parr (LYP).[31] All electrons were considered for all other atoms with the 6-31G** basis set.[32] Further DFT optimizations were carried out using the 6-311G** basis set. The energetics and mechanisms of observed cluster phase reactions are further investigated based on optimized structures and their corresponding energies for reactants and products.

4.4. Results and Discussion

4.4.1 Cluster Formation and Reactions. The observed clusters of small dicarboxylate anions are summarized in Table 1 along with their reactions. A series of intense peaks of singly charged proton-free sodiated dicarboxylate clusters are observed in the ESI mass spectra (e.g., Figure 2) of all small dicarboxylic acids (C2-C6) studied in the present chapter. The abundant clusters are generally characterized by the composition $(Na^+)_{2n+1}(dicarboxylate^{2-})_{n+1}$, where n = 1-4. The monomers, n = 0, are not observed with C2-C4 and only observed in low abundance with C5-C6. Not only the samples prepared with the mixture of sodium chloride with the acid and the disodiated carboxylate, but also all five pure dicarboxylic acid (C2-C6) samples studied here exhibit similar cluster formation in the gas phase, binding strongly with trace amounts of sodium ions present in the samples. The mass spectra of sodium salts of malonic acid and sodium salts of oxalic acid are shown in Figure 2a and 2b, respectively, as representative spectra. Because of their comparative simplicity, malonic acid clusters are discussed before presenting the data for oxalic acid clusters.

4.4.1.1 Malonic Acid (C3). A series of sodiated malonate clusters are found at m/z 273, 421, 569 and 717 that correspond to n = 1, 2, 3, and 4, respectively (Figure 2a). As seen in Figure 3a, the CID of the dimer cluster at m/z 273 (n = 1) yields one distinct product, resulting from elimination of CO_2 with the attachment of a H_2O molecule (-44 + 18 = -26 mass units). Significantly, loss of CO_2 without the incorporation of H_2O into the product is not observed. The structure of the product at m/z 247 is probed by MS^3 and MS^4 (Figure 3b-c). MS^3 shows exclusive loss of sodium acetate (CH_3CO_2Na; 82 mass units). MS^4 shows that the product from MS^3 loses NaOH (40 mass units) exclusively. Reactions similar to those observed for the dimer (n=1) characterize larger clusters (n= 2-4) as well. Reactions and proposed reaction mechanisms of sodiated malonate clusters

Figure 2. (a) ESI-MS spectrum of 180 μM disodium malonate. A series of proton-free sodiated malonate clusters, $(Na^+)_{2n+1}(malonate^{2-})_{n+1}$, where n = 1-4, are seen as dominant species. (b) ESI-MS spectrum of 90 μM oxalic acid with 90 μM sodium chloride. A series of proton-free sodiated oxalate clusters, $(Na^+)_{2n+1}(oxalate^{2-})_{n+1}$, where n = 2-5, are seen as dominant species.

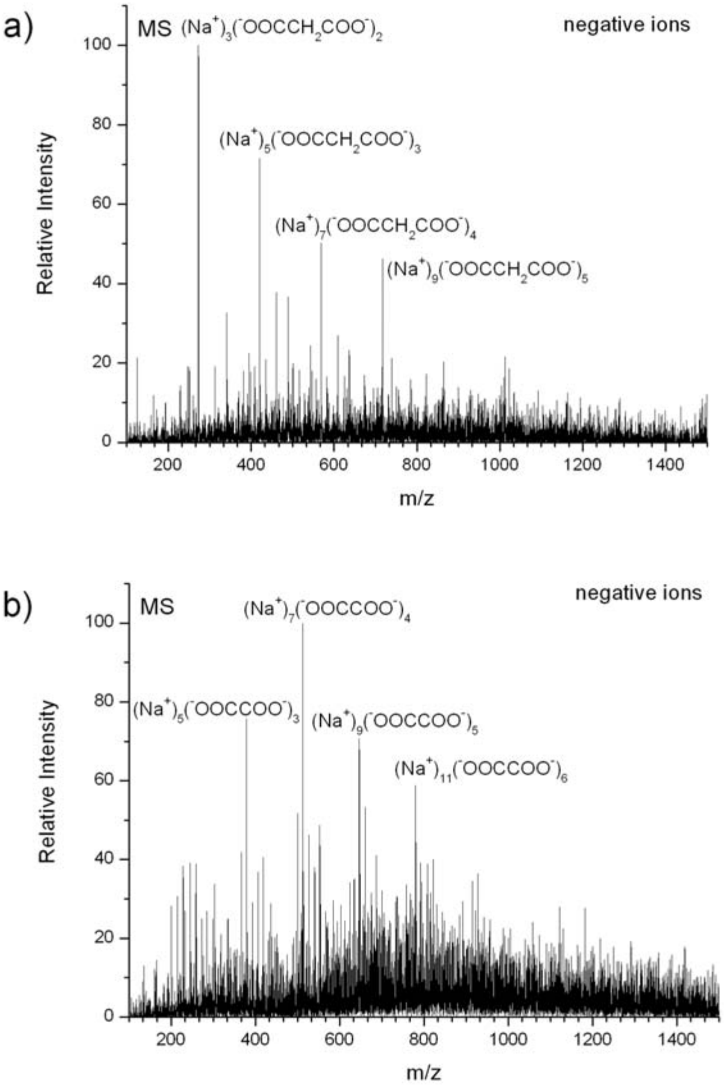

Table 1. The occurrence of sodiated clusters (C) of small dicarboxylic acid (C2-C6) and cluster phase reactions (R) in the present study. The presence of the cluster and the cluster phase reaction is indicated with empty circle (○), while absence is indicated with cross (×)

	$(Na^{+})_{2n+1}(dicarboxylate^{2-})_{n+1}$											
	n = 0		n = 1		n = 2		n =3		n = 4		n = 5	
	C	R	C	R	C	R	C	R	C	R	C	R
C2	×	×	×	×	○	○	○	○	○	○	○	○
C3	×	×	○	○	○	○	○	○	○	○	×	×
C4	×	×	○	○	○	×	○	×	○	×	×	×
C5	○	×	○	○	○	×	○	×	○	×	×	×
C6	○	×	○	×	○	×	○	×	○	×	×	×

Figure 3. (a) CID spectrum of the proton-free sodiated malonate cluster, $(Na^+)_3(malonate^{2-})_2$, showing exclusive loss of 26 mass units. (b) MS^3 spectrum of the m/z 247 product of MS^2 shows exclusive loss of CH_3COONa (-82 mass units). (c) MS^4 spectrum of the m/z 165 product of MS^3 exclusively loses NaOH (-40 mass units).

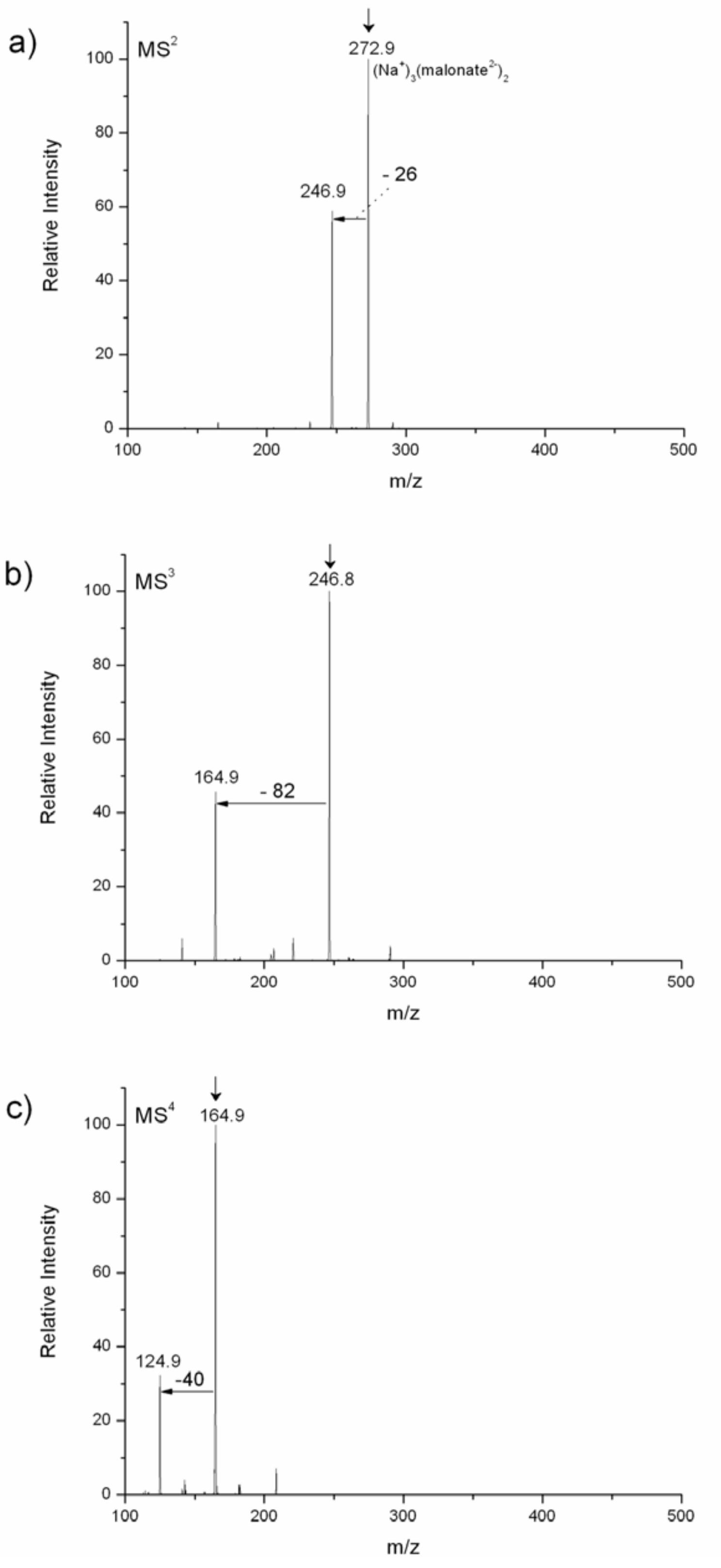
a)
MS^2
272.9
(Na$^+$)$_3$(malonate^{2-})$_2$
- 26
246.9
Relative Intensity
0
20
40
60
80
100
100
200
300
400
500
m/z
b)
MS^3
246.8
164.9
- 82
Relative Intensity
0
20
40
60
80
100
100
200
300
400
500
m/z
c)
MS^4
164.9
124.9
-40
Relative Intensity
0
20
40
60
80
100
100
200
300
400
500
m/z

Scheme 2. Reactions of sodiated malonate clusters with water molecules via CID. Product is probed by MS^3 and MS^4.

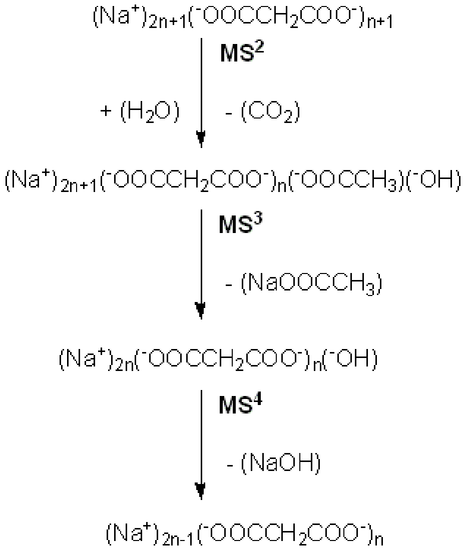

Scheme 3. Proposed reaction mechanisms of malonate dimer with a water molecule. Reaction similar to those observed for the dimer characterizes larger clusters observed in the present study as well. Each numbered state and reaction correspond to the numbered state in Figure 7.

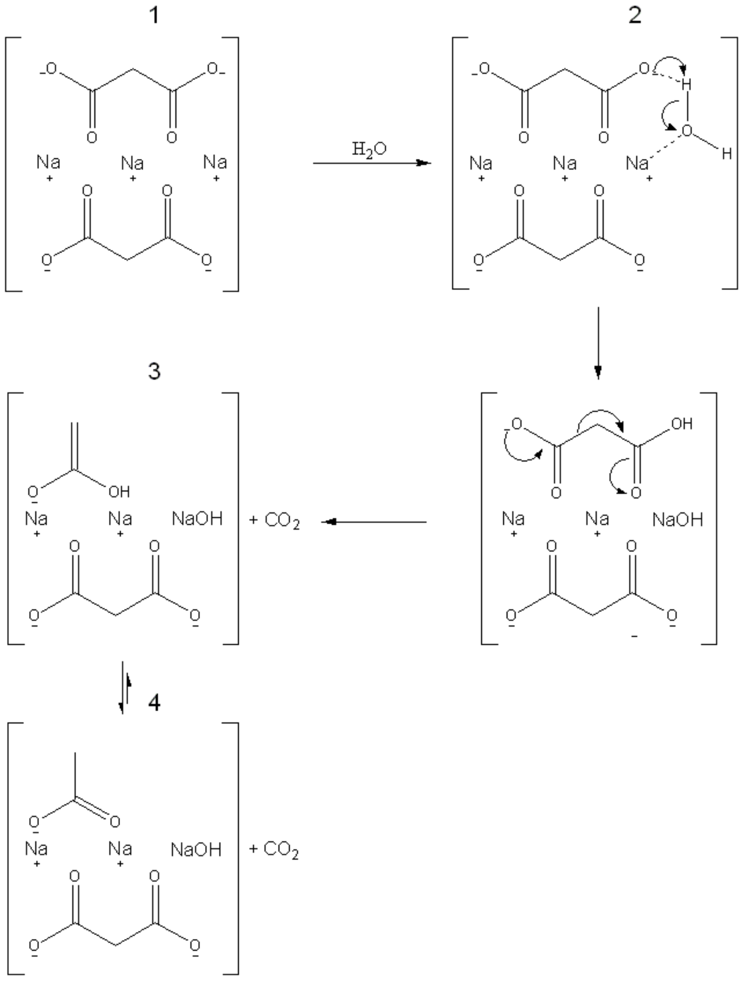

with a water molecule are shown in Schemes 2 and 3, respectively.

4.4.1.2 Oxalic Acid (C2). A series of sodiated oxalate clusters are found at m/z 379, 513, 647, and 781 that correspond to n = 2, 3, 4, and 5 respectively (Figure 2b). The CID spectrum of the trimer cluster, n = 2, (m/z 379) is presented in Figure 4a. The product at m/z 245 (Figure 4a) results from loss of a monomer, $(Na^+)_2(oxalate^{2-})$. Three other distinct products are observed at m/z 353, m/z 325, and m/z 285 (Figure 4a), in analogy to the reactions observed for sodiated malonate clusters. The structures of these products are probed by MS^3. MS^3 of the ion at m/z 353 shows a major product at m/z 285 which is yielded by the loss of sodium formate (HCO_2Na; 68 mass units, Figure 4b). Two minor products at m/z 313 and m/z 245 are also observed from MS^3 of the ion. The product at m/z 313 results from the loss of sodium hydroxide (NaOH; 40 mass units). The losses of HCO_2Na and NaOH suggest that the ion at m/z 353 from MS^2 contains a formate ion and a hydroxide ion. The product at m/z 245, which is yielded by the loss of HCO_2Na and NaOH together (108 mass units), confirms this analysis. The structure suggested for the cluster ion at m/z 353 in the MS^2 spectrum is $(Na^+)_5(oxalate^{2-})_2(formate^-)(OH^-)$, formed in conjunction with CO_2 loss from a doubly deprotonated oxalate ion in the cluster via CID. To account for the stoichiometry of the observed products, it is further inferred that the collisionally activated cluster has picked up a water molecule that donates a proton to the oxalate anion concomitant with the formation of a hydroxide ion in the cluster. The product ion at m/z 325 from MS^2 is, then, determined as $(Na^+)_5(oxalate^{2-})_2(OH^-)_2$ based on the analysis of MS^3 spectrum shown in Figure 4c. The product ion at m/z 285 resulting from the loss of sodium hydroxide (NaOH; 40 mass units) in the MS^3 spectrum of m/z 325 (Figure 4c) is also observed in the MS^3 spectrum of the ion m/z 353 (Figure 4b). The product ion at m/z 245 from MS^3 of m/z 325 results from the loss of two sodium

Figure 4. (a) CID spectrum of the proton-free sodiated oxalate cluster, $(Na^+)_5(oxalate^{2-})_3$, showing four distinct products including loss of sodiated monomer at m/z 245. Decarboxylation of the cluster with a water molecule attachment (-44 + 18 = -26 mass units) is shown at m/z 353. The product of neutral oxalic acid elimination concomitant with attachment of two water molecules (-90 + 36 = -54 mass units) is shown at m/z 325. The product of elimination of sodium oxalate concomitant with a water molecule attachment (-112 + 18 = -94 mass units) is shown at m/z 285. (b) MS^3 spectrum of the product at m/z 353 shows competitive loss of NaOH (-40 mass units) and HCO_2Na (-68 mass units). The loss of combined NaOH and HCO_2Na (-108 mass units) is also observed. (c) MS^3 spectrum product at m/z 325 shows competitive loss of NaOH (-40 mass units) and 2NaOH (-80 mass units).

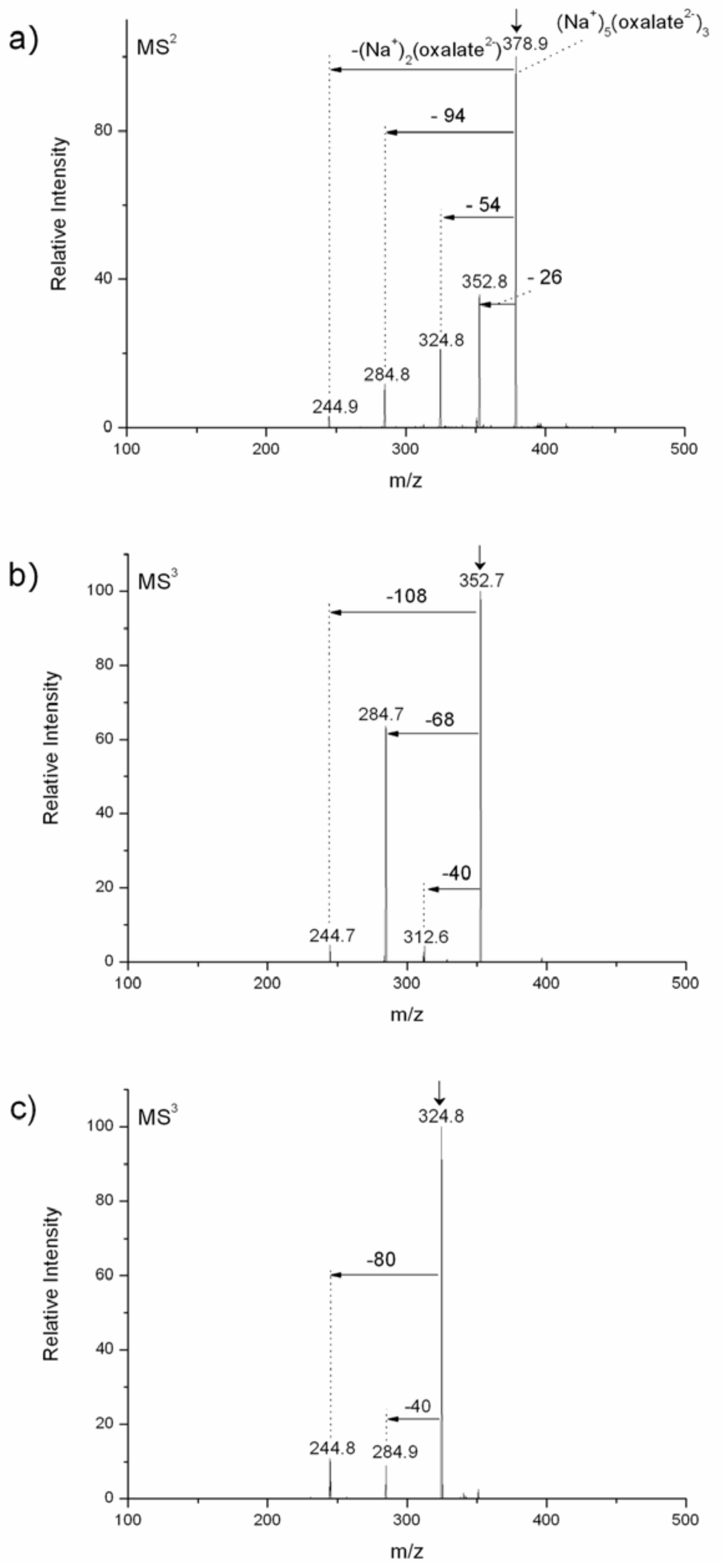
a)
MS^2
(Na$^+$)$_5$(oxalate^{2-})$_3$
-(Na$^+$)$_2$(oxalate^{2-})
378.9
- 94
- 54
- 26
352.8
324.8
284.8
244.9
Relative Intensity
0
40
80
100
200
300
400
500
m/z
b)
MS^3
352.7
-108
284.7
-68
-40
244.7
312.6
Relative Intensity
0
20
40
60
80
100
100
200
300
400
500
m/z
c)
MS^3
324.8
-80
-40
244.8
284.9
Relative Intensity
0
20
40
60
80
100
100
200
300
400
500
m/z

Scheme 4. Reactions of sodiated oxalate clusters with water molecules via CID. Yielded products are probed by MS^3 and MS^4.

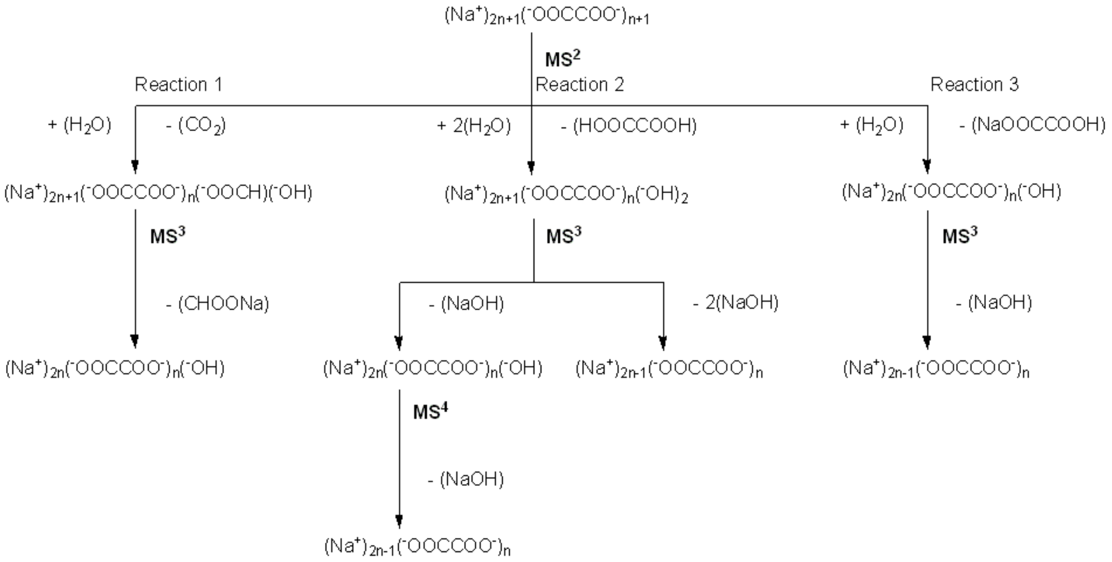

Scheme 5. Proposed reaction mechanisms of oxalate trimers with water molecules. Reactions similar to those observed for the trimer also characterize larger clusters observed in the present study. Each numbered state and reaction correspond to the numbered state and reaction in Figure 7.

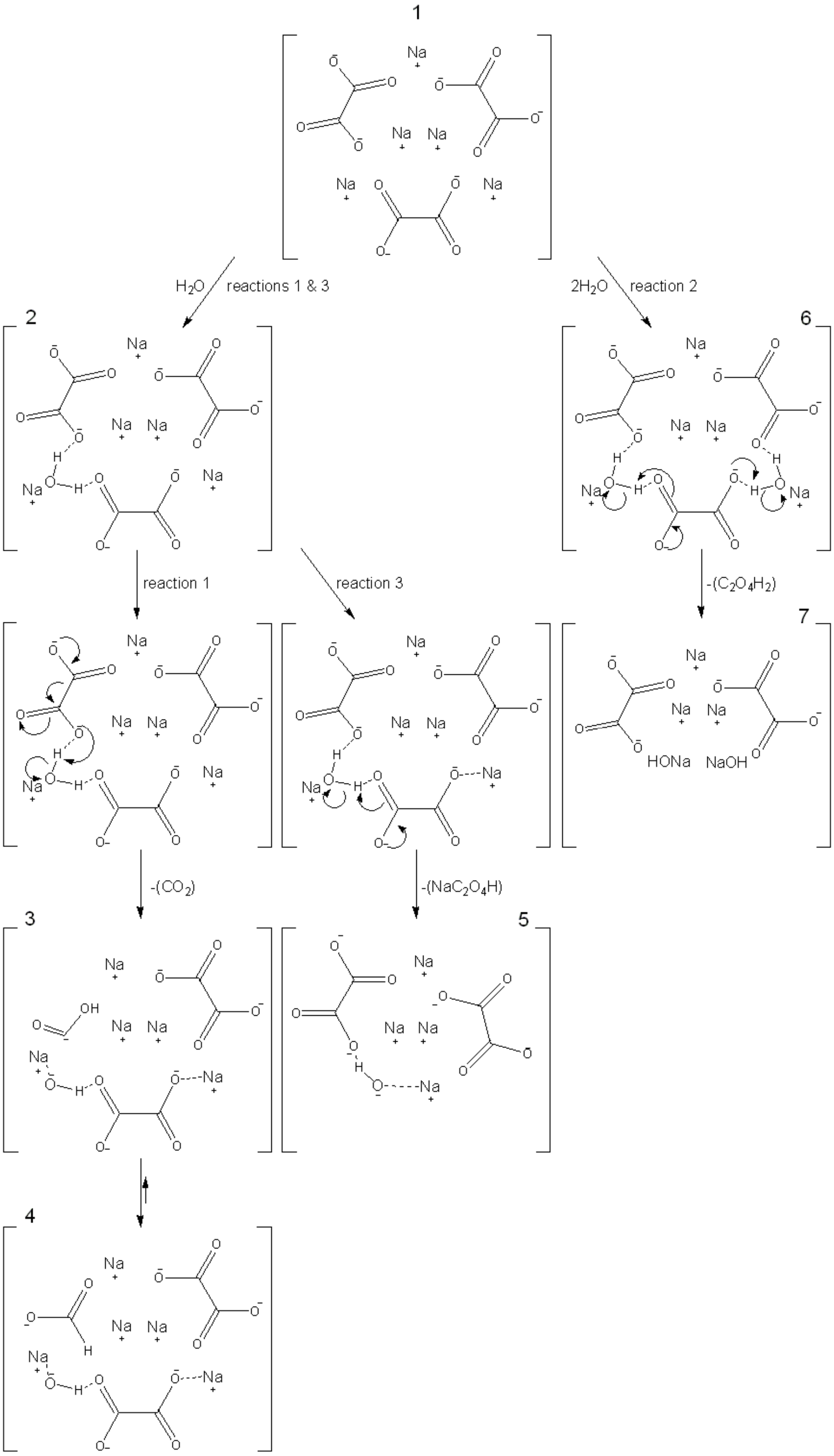
1
H_2O
reactions 1 & 3
$2H_2O$
reaction 2
2
6
reaction 1
reaction 3
$-(C_2O_4H_2)$
7
HONa
NaOH
$-(CO_2)$
$-(NaC_2O_4H)$
3
5
4

hydroxides (2NaOH; 80 mass units). The product structure at m/z 285 is analyzed as $(Na^+)_4(oxalate^{2-})_2(OH^-)$, which results from the elimination of sodium oxalate (HO_4C_2Na; 112 mass units) concomitant with attachment of a water molecule (18 mass units, Figure 4a). Reactions similar to those observed for the trimer (n = 2) characterize larger clusters (n = 3-5). Observed reactions of sodiated collisionally activated oxalate clusters with water molecules are summarized in Scheme 4.

Based on the product ions from the product at m/z 325 and m/z 285 from MS^2 and analysis of MS^3, we can conclude that water molecules present at low pressure in the ion trap react with excited dicarboxylate anions, and facilitate dissociation of the acid in a process initiated by proton transfer. The product at m/z 325 results from the loss of neutral oxalic acid ($C_2O_4H_2$; 90 mass units) concomitant with attachment of two H_2O molecules (36 mass units). The product at m/z 285 is yielded by the loss of sodium oxalate (NaC_2O_4H; 112 mass units) following interaction with a H_2O molecule. Notably, without the inference of collisions with water molecules, there is no source of protons in the clusters to form neutral oxalic acid or neutral sodium oxalate. The mechanism proposed for this process is shown in Scheme 5.

4.4.1.3 Longer Dicarboxylic Acids (C4-C6) The mass spectra of sodium salts of succinic acid, glutaric acid, and adipic acid are shown in Figures 5a, 5b, and 5c, respectively. The CID spectra of clusters of succinate, glutarate, and adipate (C4-C6) show generally the loss of $(Na^+)_2(dicarboxyate^{2-})$. However, the dimers, n=1, of sodiated succinate, $(Na^+)_3(succinate^{2-})_2$, and sodiated glutarate, $(Na^+)_3(glutarate^{2-})_2$, exhibit exceptional dissociation pathways (Figure 6a, b). The MS^n spectra of the sodiated succinate and glutarate clusters show that only the dimers interact with water molecules

Figure 5. (a) ESI-MS spectrum of 200 μM disodium succinate. A series of proton-free sodiated succinate clusters, $(Na^+)_{2n+1}(succinate^{2-})_{n+1}$, where n = 1-4, are seen as dominant species. (b) ESI-MS spectrum of 50 μM glutaric acid with 50 μM sodium chloride. A series of proton-free sodiated glutarate clusters, $(Na^+)_{2n+1}(glutarate^{2-})_{n+1}$, where n = 0-4, are seen as dominant species. A small amount of singly deprotonated glutarate anion peak is also observed at m/z 131. (c) ESI-MS spectrum of 50 μM adipic acid with 50 μM sodium chloride. A series of proton-free sodiated adipate clusters, $(Na^+)_{2n+1}(adipate^{2-})_{n+1}$, where n = 0-4, are seen as dominant species. A small amount of singly deprotonated adipate anion peak is also observed at m/z 145.

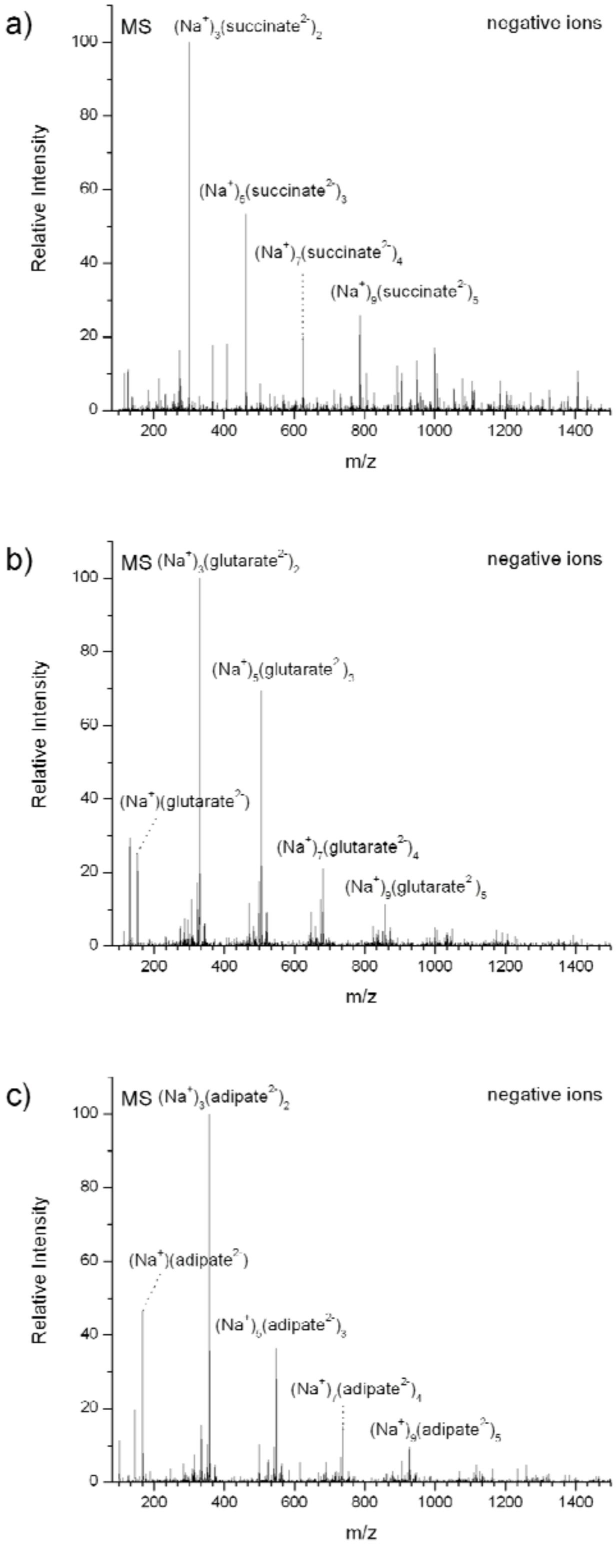
a)
MS
negative ions
$(Na^+)_3(succinate^{2-})_2$
$(Na^+)_5(succinate^{2-})_3$
$(Na^+)_7(succinate^{2-})_4$
$(Na^+)_9(succinate^{2-})_5$
Relative Intensity
m/z
0
20
40
60
80
100
200
400
600
800
1000
1200
1400
b)
MS
negative ions
$(Na^+)_3(glutarate^{2-})_2$
$(Na^+)_5(glutarate^{2-})_3$
$(Na^+)(glutarate^{2-})$
$(Na^+)_7(glutarate^{2-})_4$
$(Na^+)_9(glutarate^{2-})_5$
Relative Intensity
m/z
0
20
40
60
80
100
200
400
600
800
1000
1200
1400
c)
MS
negative ions
$(Na^+)_3(adipate^{2-})_2$
$(Na^+)(adipate^{2-})$
$(Na^+)_5(adipate^{2-})_3$
$(Na^+)_7(adipate^{2-})_4$
$(Na^+)_9(adipate^{2-})_5$
Relative Intensity
m/z
0
20
40
60
80
100
200
400
600
800
1000
1200
1400

Figure 6. (a) CID spectrum of the sodiated succinate dimer, $(Na^+)_3(succinate^{2-})_2$, showing two major products, the first (-26 mass units) resulting from decarboxylation with attachment of a water molecule and the second by loss of $(Na^+)_2(succinate^{2-})$ (-162 mass units). (b) CID spectrum of the dimer of sodiated glutarate, $(Na^+)_3(glutarate^{2-})_2$, showing two distinct products, resulting from the elimination of acrylic acid with attachment of a water molecule (-72 + 18 = -54 mass units) and by elimination of $(Na^+)_2(glutarate^{2-})$ (-176 mass units)

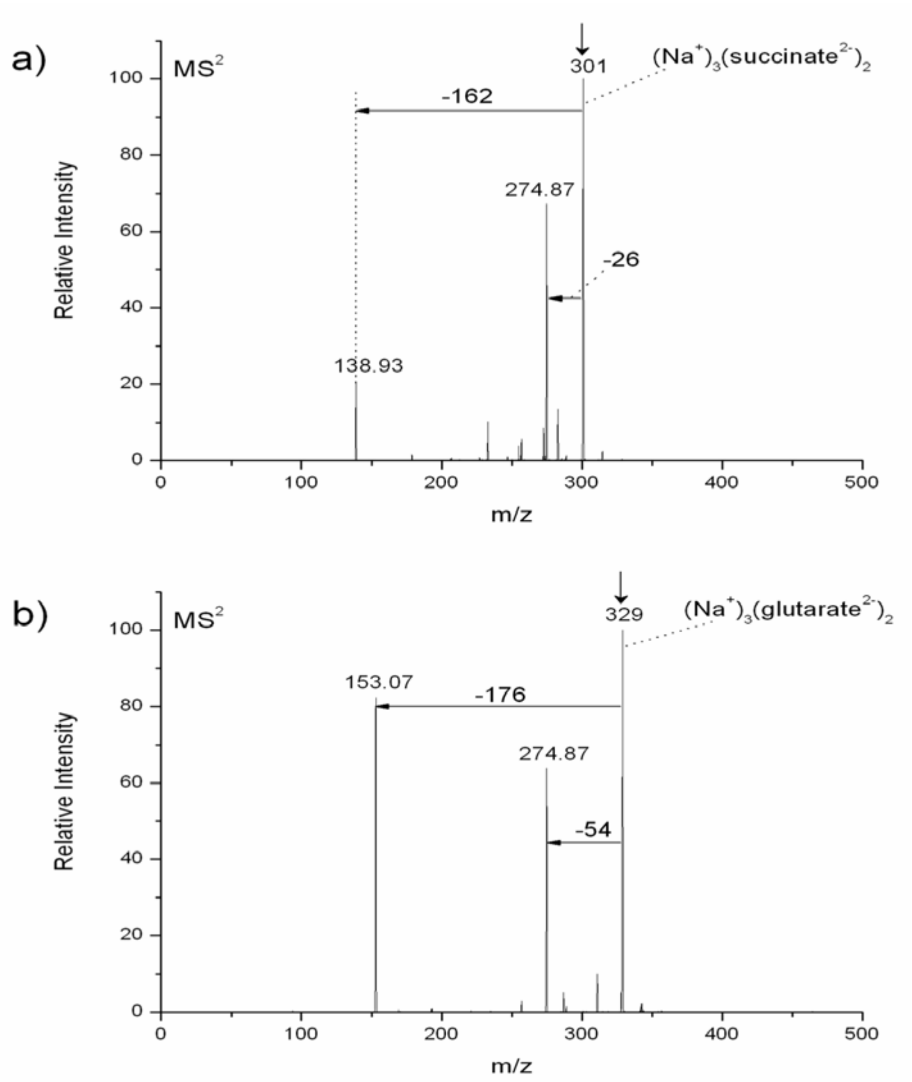

to initiate unique dissociation pathways, while larger clusters of these species dissociate by loss of the sodiated monomers. The CID of sodiated succinate dimer, n=1, yields major products at m/z 275 and m/z 139. The product at m/z 275 results from the elimination of CO_2 (44 mass units) following attachment of H_2O (18 mass units) as observed for all clusters of oxalate and malonate. The product at m/z 139 results from the loss of a monomer, $(Na^+)_2(\text{succinate}^{2-})$. The CID of the sodiated glutarate dimer, n=1, yields the major product at m/z 153, corresponding to the loss of $(Na^+)_2(\text{glutarate}^{2-})$, with an additional product at m/z 275. The product at m/z 275 is yielded by elimination of what is assumed to be acrylic acid ($H_2C{=}CHCO_2H$; 72 mass units) with attachment of H_2O (18 mass units). The elimination of acrylic acid is postulated to occur via a cyclic transition state structure formed after a water molecule interacts with an excited glutarate anion in the cluster. The proposed mechanism of the reaction is shown in Scheme 6.

Scheme 6. Proposed dissociation mechanism of a sodiated glutarate subunit in the dimmer cluster. After a water molecule donates a proton to the glutarates in the cluster, loss of acrylic acid occurs via a six-membered intramolecular cyclic transition state.

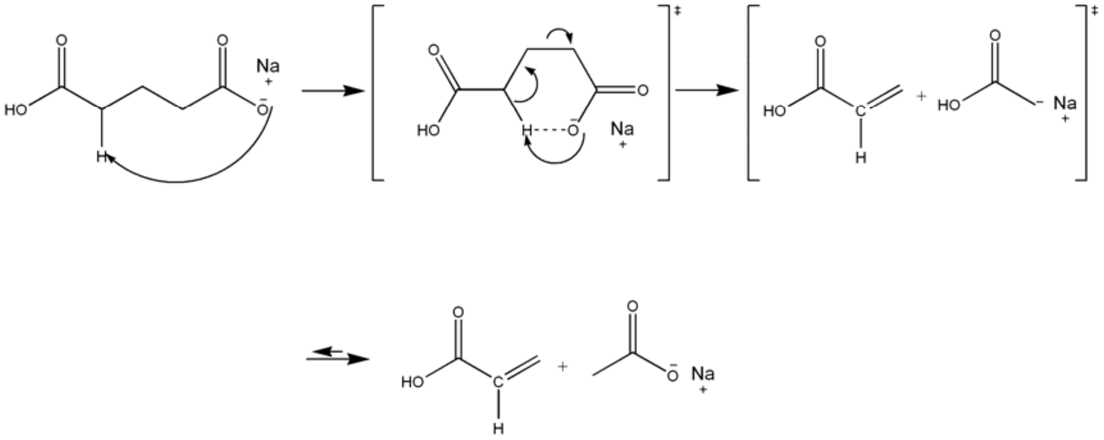

4.4.2 Theoretical Results. In the present investigation we have shown that the interaction of water molecules with collisionally activated anionic sodiated dicarboxylate clusters can trigger the decarboxylation of dicarboxylic acids within the sodiated clusters. In order to probe the mechanism and energetics of these and other cluster phase reactions, the optimized geometries of the ground state reactants and products of anionic small dicarboxylate (C2-C6) clusters with corresponding electronic energies have been investigated through the computational methods described in Section 2. Calculated changes of energy (ΔE) through the reactions of malonate dimers and oxalate trimers with water molecules are shown in Figures 7 and 8. Optimized geometries of sodiated dicarboxylate trimers and predicted water-cluster complex structures are shown in Figures 9 and 10, respectively.

4.4.2.1 Malonic acid (C3). In the proton-free sodiated malonate clusters, doubly deprotonated malonate anions are bound to sodium cations (Figure 9). DFT calculations indicate that a water molecule binds strongly to the cluster to form a complex (Figure 10). In the water-cluster complex, the oxygen atom of the water molecule interacts with a sodium cation while each hydrogen atom is bound to a carboxylate oxygen. As discussed in Section 3.1.1, the decarboxylation of the malonate anion via single water molecule attachment is observed as a facile reaction of malonate clusters (Figure 3a). The proposed malonate water-cluster complex is shown in Figure 10c. This yields the enol acetate anion with the hydroxide ion incorporated in the cluster after decarboxylation, giving the product at m/z 247 shown in Figure 3a. It is inferred that the enol acetate anion rapidly isomerizes to yield the more stable acetate ion, lowering the energy of the cluster by 20 kcal/mol for the dimer (n=1), and 32 kcal/mol for the trimer (n=2). The estimated energetics for the reaction of the malonate dimer (n=1) are shown in Figure 7.

Figure 7. Reaction coordinate diagram showing relative energies in kcal/mol for cluster phase reactions of the sodiated malonate dimer with a water molecule at the B3LYP/6-311G** level, including zero-point correction for 298.15 K obtained at the same scaled level. Barrier heights are not known. The structure of each numbered species is shown in Scheme 3.

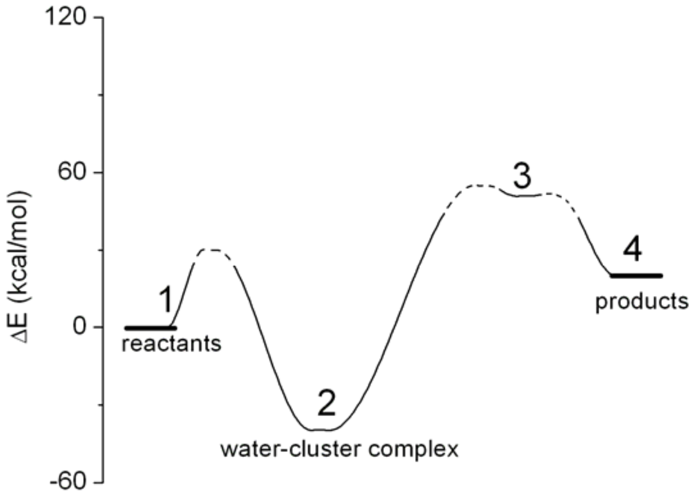

Figure 8. Reaction coordinate diagram showing relative energies in kcal/mol for cluster phase reactions of sodiated oxalate trimer with (a) a water molecule and (b) two water molecules at the B3LYP/6-311G** level, including zero-point correction for 298.15 K obtained at the same scaled level. Barrier heights are not known. The structure of each numbered species of corresponding reaction is shown in Scheme 5.

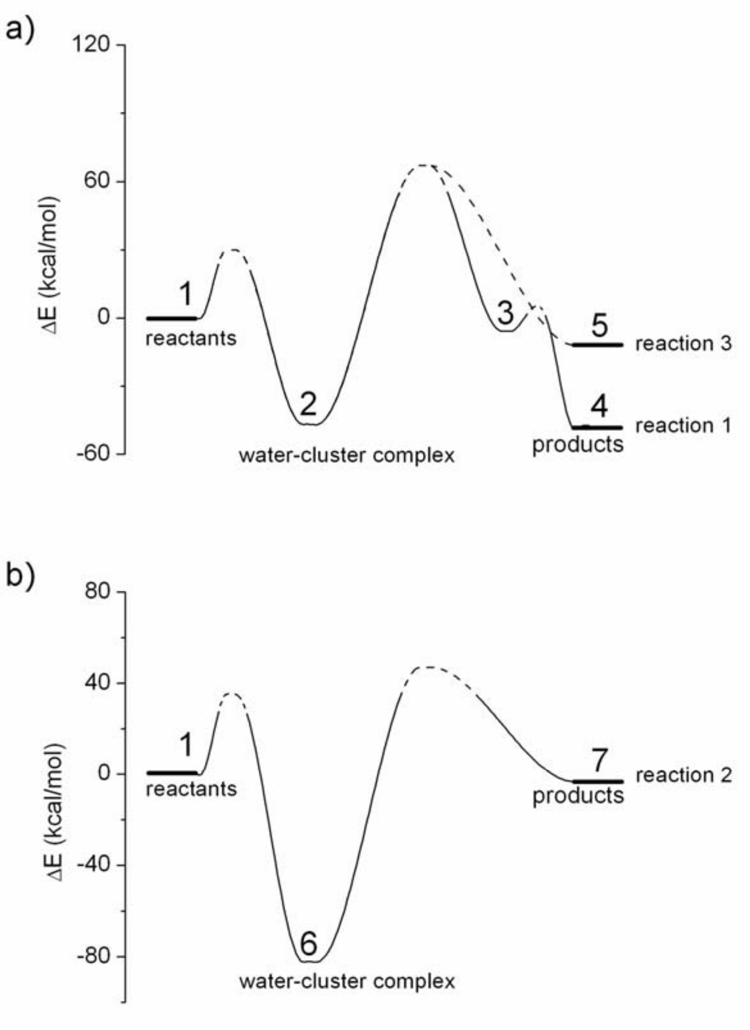

Figure 9. Optimized structures of the sodiated dicarboxylate cluster anions (n=2) using DFT at the B3LYP/6-311G** level.

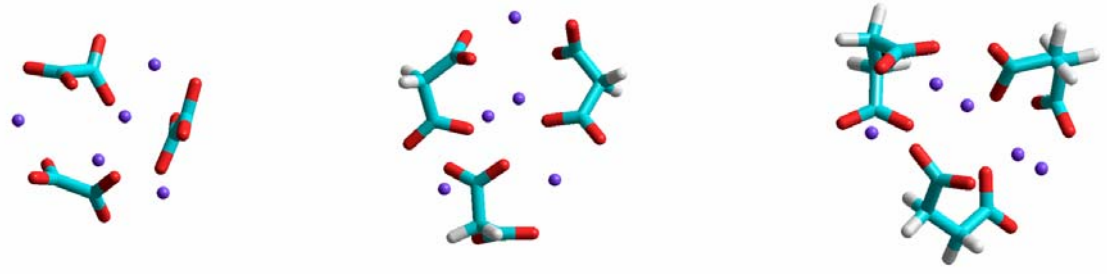

sodiated oxalate cluster sodiated malonate cluster sodiated succinate cluster

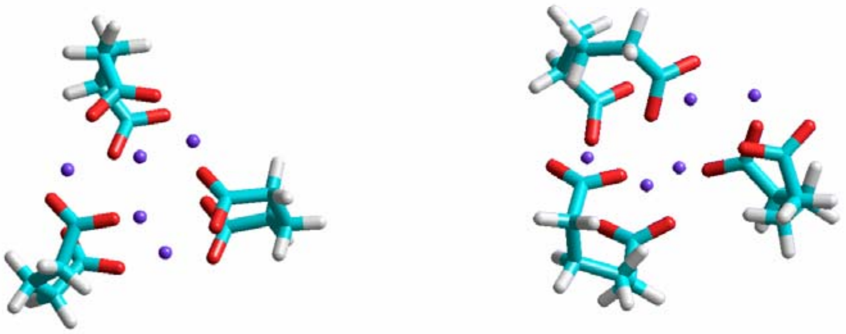

sodiated glutarate cluster sodiated adipate cluster

Figure 10. Optimized geometries of water-cluster complexes using DFT at the B3LYP/6-311G** level. (a) Water-sodiated oxalate trimer complex I with one water molecule attached. (b) Water-sodiated oxalate trimer complex II with attachment of two water molecules. (c) Water-sodiated malonate dimer complex. (d) Water-sodiated succinate dimer cluster (e) Water-sodiated glutarate dimer complex. (f) Water-sodiated adipate dimer complex. Hydrogen bonds are indicated with solid lines. Water-cluster complex formations with dimers (trimer for oxalate cluster) also characterize larger clusters.

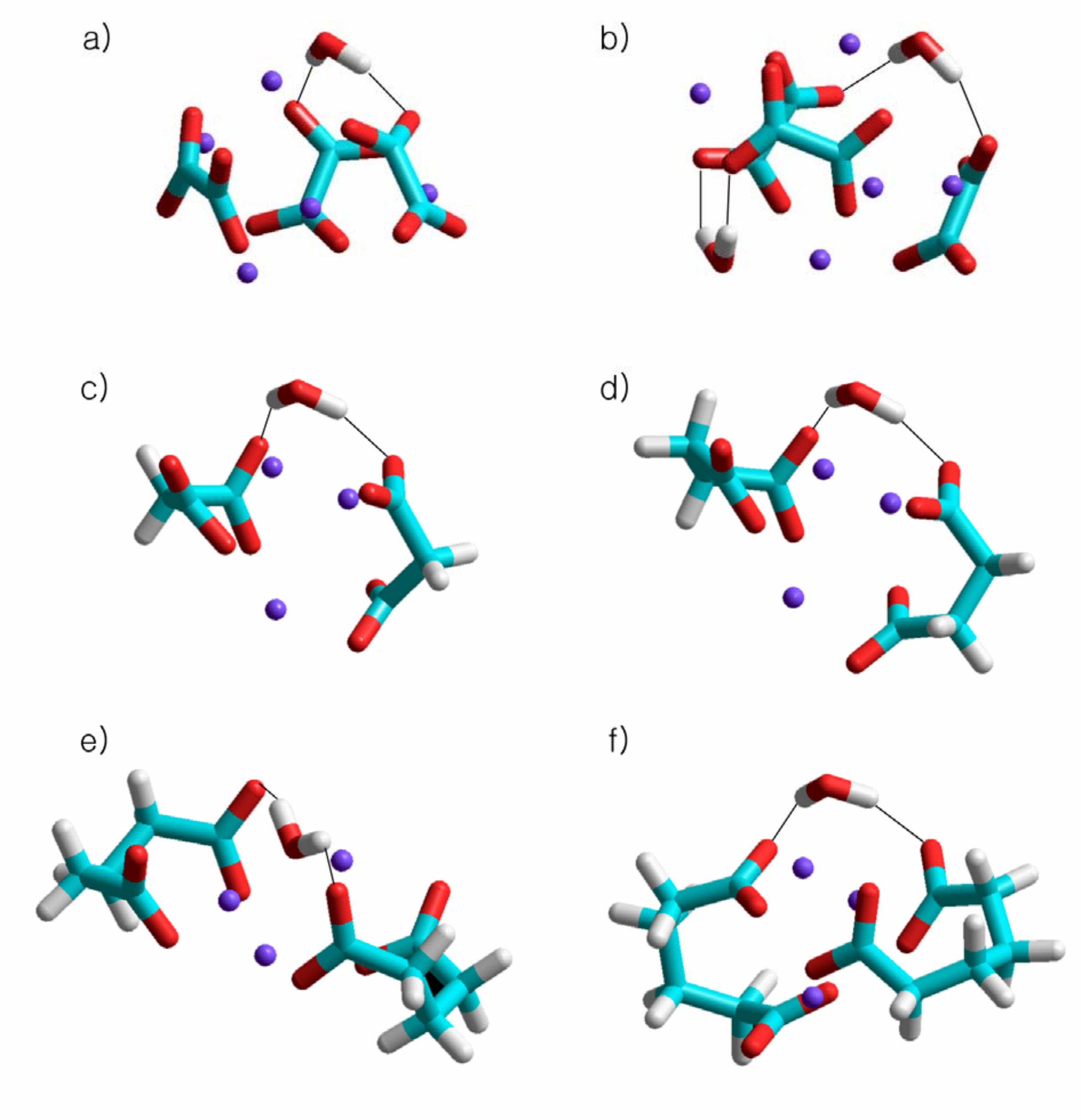
a)
b)
c)
d)
e)
f)

4.4.2.2 Oxalic Acid (C2). In analogy with the sodiated malonate clusters, doubly deprotonated oxalate anions are bound strongly to sodium cations in the sodiated oxalate clusters (Figure 9). The optimized geometries of water-oxalate cluster (n=2) complexes with one water molecule (complex I) and with two water molecules (complex II) are shown in Figure 10a and Figure 10b, respectively. Three distinct products are observed from the MS^2 spectrum in Figure 4a. Through the complex shown in Figure 10a, energetically unstable $HOOC^-$ product is expected with the hydroxide ion in the cluster after decarboxylation for the product at m/z 353 in Figure 4a (reaction 1 in Scheme 4). The rapid rearrangement of unstable $HOOC^-$ to formate (^-OOCH) is expected since this transformation lowers the energy of the cluster by 42 kcal/mol (n=2). It is inferred that sodium oxalate elimination (reaction 3 in Scheme 4, m/z 285 in Figure 4a) occurs via the same complex formed in the decarboxylation reaction. Once complexes are formed with a single water molecule (Figure 10a), two distinct products are yielded (Figure 4a) via decarboxylation (reaction 1 in Scheme 4) and sodium oxalate elimination (reaction 3 in Scheme 4). Favorable reaction energetics (Figure 8) are consistent with the observed product abundance from MS^2 (Figure 4a), where decarboxylation (reaction 1 in Scheme 4) is the dominant reaction while elimination of sodium oxalate (reaction 3 in Scheme 4) is the less favored reaction. The species resulting from the elimination of neutral oxalic acid with incorporation of two hydroxide ions in the observed product (reaction 2 in Scheme 4, m/z 325 in Figure 4a) is expected to also result from water complex formation involving attachment of two water molecules (Figure 10b).

4.4.2.3 Longer Dicarboxylic Acids (C4-C6). Optimized structures of the sodiated dicarboxylate clusters of longer dicarboxylic acids (C4-C6) show cluster structures similar to those of oxalic acid (C2) and malonic acid (C3). However, the more flexible longer dicarboxylate anions allow the carboxylate functional groups to group more tightly with the sodium cations toward the center of the aggregate (Figure 9). An interesting question to consider relating to the cluster phase chemistry of the sodiated dicarboxylate clusters is the following. Why do complex reactions initiated by interaction of the vibrationally excited clusters with a water molecule occur mainly with clusters of the smallest two dicarboxylates (C2 and C3) while longer dicarboxylate (C4-C6) clusters generally exhibit sequential loss of the monomeric $(Na^+)_2(dicarboxylate^{2-})$ subunits? Calculated binding energies of the monomers, $(Na^+)_2(dicarboxylate^{2-})$, in the sodiated dicarboxylate clusters, when n = 1-3, are shown in Figure 11. Excluding oxalate, for a particular acid the incremental binding energy decreases with increasing cluster size. For a given cluster size, again excluding oxalate, there is a decrease of approximately 6 kcal/mol for each methylene added to the acid. The major attractive interaction that contributes to the stability of carboxylate clusters is the coulombic attraction between the charged constituents. While this is greatest for the smaller members of the series that can pack closely together, the methylene chain allows additional flexibility to optimize attraction. These two factors appear to reach an optimum balance in the case of the malonate and succinate dimers, which have the highest binding energy among all dicarboxylate clusters examined. With larger members of the series there is a decreasing incremental increase in total coulombic attraction as carboxylate units are added to the cluster. Based on the observed reactions of the smaller acids, it appears ~70 kcal/mol or larger binding energy for a monomer, $(Na^+)_2(dicarboxylate^{2-})$, is required to facilitate more complex cluster phase reactions (Figure 11). Strong binding energies of succinate (C4) and glutarate (C5) dimers (Figure 11) allow exceptional cluster phase reactions of these dimers with water molecules, as discussed above in Section 3.1.3. However, adipate

Figure 11. Plots of calculated binding energies of sodiated monomers, $(Na^+)_2(dicarboxylate^{2-})$, in the clusters, $(Na^+)_{2n+1}(dicarboxylate^{2-})_{n+1}$ observed in this study (except the oxalate dimer), versus number of dicarboxylic acid carbons.

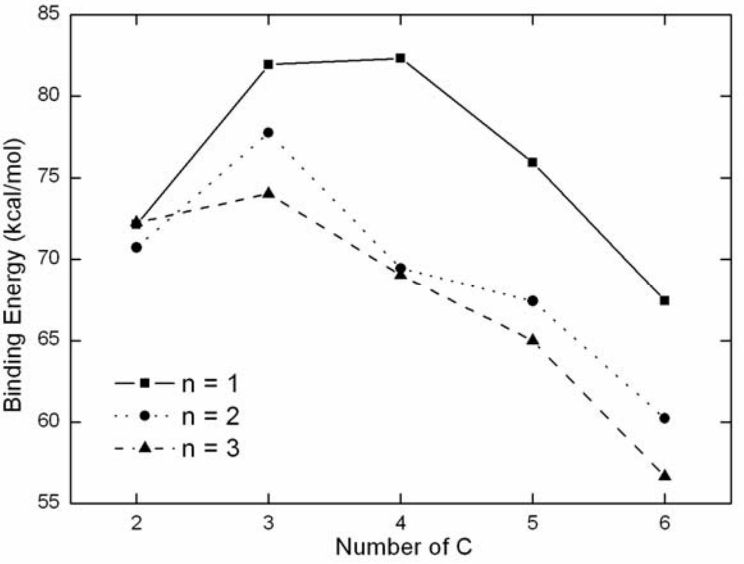

(C6) dimer, which has a binding energy less than 70 kcal/mol, only exhibits monomeric dissociation as observed with larger adipate clusters.

As noted in the introduction, previous studies have suggested that water can act as a catalyst to modify energetics of reactions important in atmospheric chemistry.[16,17,33] The water molecule is a true catalyst and is not incorporated into the products. In contrast, in the current study we have shown that water molecules facilitate complex molecular rearrangements while becoming incorporated in the reaction products rather than acting as true catalysts. Water molecules participate in the reaction by introducing new, energetically favorable reaction pathways.

4.5. Conclusion

Cluster phase reactions of singly charged anionic sodiated dicarboxylate clusters with water molecules are demonstrated in the present chapter for the first time. While clusters of longer dicarboxylate ions (C4-C6) generally exhibit sequential loss of disodium dicarboxylate moieties, all oxalate (C2) and malonate (C3) clusters and dimers (n=1) of succinate (C4) and glutarate (C5) activated by CID exhibit chemical reactions with water molecules. Water molecules donate protons to dicarboxylate anions, initiating chemical processes including decarboxylation of the diacid. Theoretical investigations of the clusters using DFT show that the binding energy of the clusters plays a key role in the cluster phase reactions. Clusters that preferentially react with water molecules typically have binding energies greater than ~70 kcal/mol with respect to elimination of a disodium dicarboxylate subunit.

4.6. Acknowledgment

The research described in this chapter was carried out at the Beckman Institute and Jet Propulsion Laboratory of the California Institute of Technology. We appreciate the support provided by the Mass Spectrometry Resource Center in the Beckman Institute, California Institute of Technology. Partial support was also provided by the National Science Foundation (NSF) under grant No. CHE-0416381. We greatly appreciate the support and critical discussion of Drs. Isik Kanik, Luther W. Beegle, Paul V. Johnson, and Charles P. Malone at Jet Propulsion Laboratory, California Institute of Technology.

4.7. References

(1) Kawamura, K.; Kaplan, I. R. *Environ. Sci. Technol.* **1987**, 21, 105.

(2) Kawamura, K.; Kasukabe, H.; Barrie, L. A. *Atmos. Environ.* **1996**, 30, 1709.

(3) Kawamura, K.; Sakaguchi, F. *J. Geophys. Res.* **1999**, 104, 3501.

(4) Kawamura, K.; Umemoto, N.; Mochida, M.; Bertram, T.; Howell, S.; Huebert, B. J. *J. Geophys. Res.* **2003**, 108.

(5) Kawamura, K.; Usukura, K. *Journal of Oceanography* **1993**, 49, 271.

(6) Sempere, R.; Kawamura, K. *Global Biogeochem. Cycles* **200**3, 17, 1069.

(7) Sempere, R.; Kawamura, K. *Atmos. Environ.* **1994**, 28, 449.

(8) Gao, S.; Ng, N. L.; Keywood, M.; Varutbangkul, V.; Bahreini, R.; Nenes, A.; He, J. W.; Yoo, K. Y.; Beauchamp, J. L.; Hodyss, R. P.; Flagan, R. C.; Seinfeld, J. H. *Environ. Sci. Technol.* **2004**, 38, 6582.

(9) Gao, S.; Keywood, M.; Ng, N. L.; Surratt, J.; Varutbangkul, V.; Bahreini, R.; Flagan, R. C.; Seinfeld, J. H. *J. Phys. Chem. A* **2004**, 108, 10147.

(10) Crahan, K. K.; Hegg, D.; Covert, D. S.; Jonsson, H. *Atmos. Environ.* **200**4, 38, 3757.

(11) Castleman, A. W.; Bowen, K. H. *J. Phys. Chem.* **1996**, 100, 12911.

(12) Gard, E. E.; Kleeman, M. J.; Gross, D. S.; Hughes, L. S.; Allen, J. O.; Morrical, B. D.; Fergenson, D. P.; Dienes, T.; Galli, M. E.; Johnson, R. J.; Cass, G. R.; Prather, K. A. *Science* **1998**, 279, 1184.

(13) Woodcock, A. H. *Journal of Meteorology* **1953**, 10, 362.

(14) Bock, C. W.; Redington, R. L. *J. Chem. Phys*. **1986**, 85, 5391.

(15) Huang, C. L.; Wu, C. C.; Lien, M. H. *J. Phys. Chem. A* **1997**, 101, 7867.

(16) Staikova, M.; Oh, M.; Donaldson, D. J. *J. Phys. Chem. A* **2005**, 109, 597.

(17) Staikova, M.; Donaldson, D. *J. Physics and Chemistry of the Earth. C* **2001**, 26, 473.

(18) Bishenden, E.; Donaldson, D. J. *J. Phys. Chem. A* **1998**, 102, 4638.

(19) Donaldson, D. J. *J. Phys. Chem. A* **1999**, 103, 62.

(20) Hodyss, R.; Cox, H. A.; Beauchamp, J. L. *J. Phys. Chem. A* **2004**, 108, 10030.

(21) Julian, R. R.; Beauchamp, J. L. Int. *J. Mass Spectrom*. **2003**, 227, 147.

(22) Cox, H. A.; Hodyss, R.; Beauchamp, J. L. *J. Am. Chem. Soc*. **2005**, 127, 4084.

(23) Gronert, S.; Fagin, A. E.; Okamoto, K. *J. Am. Soc. Mass. Spectrom*. **2004**, 15, 1509.

(24) Gronert, S.; Fong, L. M. *Aust. J. Chem*. **2003**, 56, 379.

(25) Gronert, S. *Acc. Chem. Res*. **2003**, 36, 848.

(26) Gronert, S.; Azebu, *J. Org. Lett*. **1999**, 1, 503.

(27) Danielson, P. *R & D Magazine* **2001**, 43, 66.

(28) Hobson, J. P. *J. Vac. Sci. Tech. A* **2003**, 21, S7.

(29) Shukla, A.; Futrell, J. H. *J. Mass Spectrom.* **2000**, 35, 1069.

(30) Becke, A. D. *J. Chem. Phys.* **1993**, 98, 5648.

(31) Lee, C. T.; Yang, W. T.; Parr, R. G. *Phys. Rev. B* **1988**, 37, 785.

(32) Harihara.Pc; Pople, J. *A. Chem. Phys. Letters* **1972**, 16, 217.

(33) Canagaratna, M.; Phillips, J. A.; Ott, M. E.; Leopold, K. R. *J. Phys. Chem. A* **1998**, 102, 1489.